AGU ADVANCING EARTH AND SPACE SCIENCE

Geophysical Research Letters

RESEARCH LETTER
10.1029/2020GL088890

Contrasting Recent Trends in Southern Hemisphere Westerlies Across Different Ocean Basins

Darryn W. Waugh[1,2], **Antara Banerjee**[3,4], **John C. Fyfe**[5], **and Lorenzo M. Polvani**[6]

[1]Department of Earth and Planetary Sciences, Johns Hopkins University, Baltimore, MD, USA, [2]School of Mathematics and Statistics, University of New South Wales, Sydney, New South Wales, Australia, [3]Cooperative Institute for Research in Environmental Sciences, University of Colorado Boulder, Boulder, CO, USA, [4]Chemical Sciences Laboratory, National Oceanic and Atmospheric Administration, Boulder, CO, USA, [5]Canadian Centre for Climate Modelling and Analysis, Environment and Climate Change Canada, Victoria, British Columbia, Canada, [6]Department of Applied Physics and Applied Mathematics, Columbia University, New York, NY, USA

Abstract Many studies have documented the trends in the latitudinal position and strength of the midlatitude westerlies in the Southern Hemisphere. However, very little attention has been paid to the longitudinal variations of these trends. Here, we specifically focus on the zonal asymmetries in the southern hemisphere wind trends between 1980 and 2018. Meteorological reanalyses show a large strengthening and a statistically insignificant equatorward shift of peak near-surface winds over the Pacific, in contrast to a weaker strengthening and significant poleward shift over the Atlantic and Indian Ocean sectors. The reanalysis trends fall within the ensemble spread for historical climate model simulations, showing that climate models are able to capture the observed trends. Climate model simulations indicate that the differential movement of the peak westerlies is a manifestation of internal variability and is not a forced response. Implications of these asymmetries for other components of the climate system are discussed.

Plain Language Summary The band of strong westerly winds in middle latitudes, which are often referred to as the midlatitude jet stream, influence not only temperature, regional storms, and precipitation but also the ocean circulation and amount of carbon and heat entering the oceans. In recent years, much attention has been paid to the observed strengthening and poleward shift of the Southern Hemisphere midlatitude jet. However, nearly all the focus has rested on trends in longitudinally averaged winds. Here we specifically focus on the longitudinal variations in trends over the last four decades. Observationally based data show that while the peak annual-averaged winds over the Atlantic and Indian Oceans have moved toward the South Pole, there has been an insignificant shift toward the equator for the peak winds over the Pacific Ocean. Simulations with climate models indicate that the underlying cause of this differential movement of the peak winds is internal atmospheric variability, and not a response to human activities. The longitudinal variations in the wind trends may have consequences for ocean gyre circulations and associated transport of heat and carbon into the oceans.

Key Points:
- There are substantial zonal variations in past trends in the magnitude and latitude of the peak Southern Hemisphere zonal winds
- Only over the Atlantic and Indian Oceans have peak winds shifted poleward, with an equatorward (yet insignificant) shift over the Pacific
- Climate model simulations indicate that the differential movement of the westerlies is due to internal atmospheric variability

Supporting Information:
- Supporting Information S1

Correspondence to:
D. W. Waugh,
waugh@jhu.edu

Citation:
Waugh, D. W., Banerjee, A., Fyfe, J. C., & Polvani, L. M. (2020). Contrasting recent trends in Southern Hemisphere westerlies across different ocean basin. *Geophysical Research Letters*, *47*, e2020GL088890. https://doi.org/10.1029/2020GL088890

Received 19 MAY 2020
Accepted 6 SEP 2020
Accepted article online 9 SEP 2020

1. Introduction

The near-surface westerlies are a dominant feature of the midlatitude atmospheric circulation of the Southern Hemisphere (SH), influencing temperature, regional storms, and precipitation (e.g., Hendon et al., 2007; Thompson & Wallace, 2000). In addition, these winds play a major role in driving the ocean circulation, and the uptake of carbon and heat (e.g., Hall & Visbeck, 2002; Sen Gupta & England, 2006; Toggweiler & Russell, 2008). In recent years, much attention has been paid to an intensification and poleward shift of these westerlies over the last four decades (e.g., Swart & Fyfe, 2012; Swart et al., 2015; Thomas et al., 2015; Thompson et al., 2011), the connections with the southern annular mode (e.g., Fogt & Marshall, 2020), and the wider impacts on the atmosphere and oceans (e.g., Le Quere et al., 2007; Roemmich et al., 2007; Waugh et al., 2013). However, this attention has focused primarily on changes in the zonal-mean winds, and longitudinal variations have been largely overlooked. While changes in the mean meridional circulation (of the atmosphere and oceans) will likely be closely related to changes in the zonal-mean winds, the response of many other aspects, such as the subtropical gyre circulation and associated changes in ventilation, heat uptake, and sea level, will depend more on regional changes

(e.g., Cai et al., 2010; Jones et al., 2019; Waugh et al., 2019; Zhang et al., 2014). It is therefore important to know whether regionally averaged winds have also intensified and moved poleward.

Furthermore, most of the previous analysis of SH wind trends has been on the summer changes, when zonal-mean trends are the largest. However, the trends in annual-mean winds are likely the most relevant for ocean impacts, as the ocean response to changes in SH winds occurs over decadal or longer time scales (e.g., Waugh & Haine, 2020).

In this study, we examine the zonal asymmetries in trends in the peak near-surface zonal winds (which mark the midlatitude, eddy-driven jet) in the SH over the last four decades. Numerous studies have shown substantial differences in the variability and response to forcing between the North Pacific and North Atlantic eddy-driven jets (e.g., Barnes & Polvani, 2013; Eichelberger & Hartmann, 2007), but less it is known about whether there has been a uniform strengthening and latitudinal shift in peak winds across the southern midlatitudes. Our study extends earlier studies by Schneider et al. (2015) and Swart et al. (2015) who showed that there are spatial variations in past trends in near-surface winds, but did not examine the impact of these trends on the strength and position of the peak winds averaged over each ocean basin. Yang et al. (2020) have very recently examined zonal variations in eddy-driven jet trends, but they only considered summer trends. We show here that the winter-spring (and annual-mean) trends differ substantially from the summer trends.

We use near-surface winds from multiple meteorological reanalyses to quantify the changes since 1980 and examine the causes of these changes using multimodel ensembles from the Coupled Model Intercomparison Project phase 5 (CMIP5; Taylor et al., 2012) and large initial-condition ensembles from the Canadian Earth System Model Version 2 (CanESM2; Gagné et al., 2017). These model ensembles have been previously used to examine trends and variability in the zonal-mean atmospheric circulation (e.g., Banerjee et al., 2020; Grise et al., 2019), and we extend these studies to consider zonal variations in trends. In combination, these ensembles enable comparison with observations as well as examination of the role atmosphere-ocean coupling and of different anthropogenic forcings.

2. Methods

We examine recent changes in the SH winds using three atmospheric reanalysis products: ERA-I (Dee et al., 2011) with horizontal resolution of 0.7° latitude × 0.7° longitude; JRA-55 (Kobayashi et al., 2015) with resolution 2.5° × 2.5°; and MERRA2 (Gelaro et al., 2017) with resolution 0.5° × 0.625°. We select these as older generation reanalyses have been shown to yield spurious trends and poorer agreement for metrics of the midlatitude jet (e.g., Grise et al., 2019; Swart et al., 2015). We focus on the period from 1980 to 2018, which is common to all these reanalyses.

Two different types of model ensembles are used to ascertain the causes of the trends seen in the reanalyses. The first type are multimodel ensembles using climate models that participated in CMIP5. The ensembles examined include the following:

- "historical" simulations driven by all-known natural and anthropogenic forcings covering the period 1850–2005,
- atmosphere-only "AMIP" simulations driven by all forcings between 1979–2005 but with observed sea surface temperatures (SSTs) and sea ice concentrations,
- preindustrial control (piControl) simulations at constant 1850 forcings, and
- "4xCO2" simulations with an instantaneous quadrupling of atmospheric CO_2 from piControl conditions.

For each model and scenario, we analyze only the first ensemble member ("r1i1p1"), in order to weigh all models equally. We use monthly mean model output from 20 models, for which we have all simulations (see supporting information Table S1); this is a subset of the 23 models considered in several earlier studies of changes in zonal-mean winds, for example, Grise and Polvani (2014, 2016) and Waugh et al. (2018). We analyze trends over the 1980–2005 period for the CMIP5 historical and AMIP simulations, which end in 2005. For the response to 4xCO2, we average of the last 50 years of the 4xCO2 simulation and take the difference from the piControl climatology.

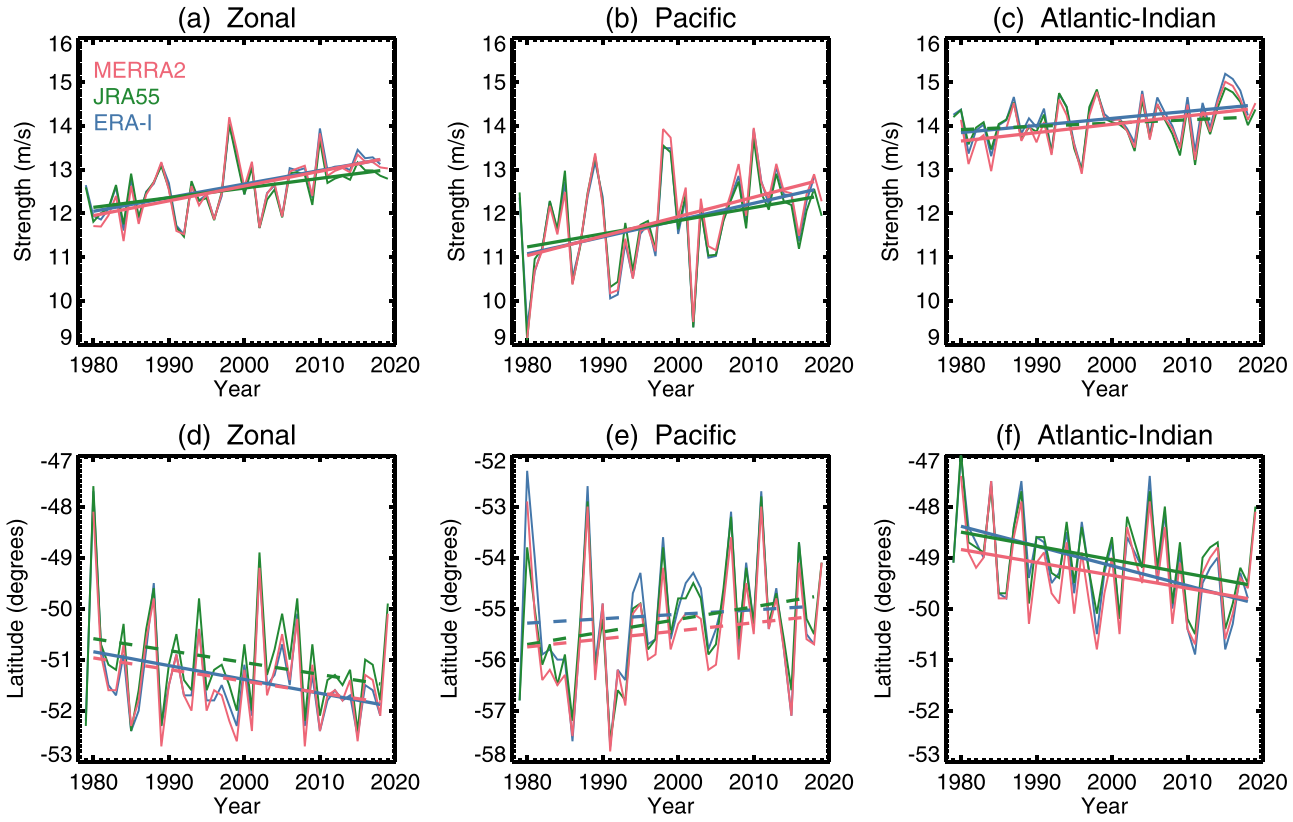

Figure 1. Time series of (a–c) strength and (d–f) position of peak winds, for (a, d) zonal-mean, (b, e) Pacific, and (c, f) Atlantic-Indian averages. Different colors for MERRA2, JRA55, and ERA-I reanalyses, with lines show 1980–2018 linear trends (solid if significant at 95% confidence level). Note the different *y* axis in (d)–(f).

The second type of ensembles are large (50-member) initial-condition ensembles of simulations from a single model, CanESM2. The atmospheric component of this model has horizontal resolution of 2.8° latitude × 2.8° longitude, with 35 vertical levels. For this model there are four different ensembles:

- a historical all-forcing ensemble using the same forcing as the CMIP5 historical simulations;
- a single-forcing ensemble where stratospheric ozone ("OZ") is the only time varying forcing;
- a single-forcing anthropogenic aerosols ("AA") ensemble; and
- a single-forcing natural, volcanic and solar, ("NAT") forcing ensemble.

We use the CanESM2 rather than other single model large ensembles as the above four different ensembles have been performed with CanESM2, which allows us to isolate the role of different external forcings. As with the CMIP5 ensembles, we analyze the 1979–2005 period.

In both reanalyses and model output, we examine the monthly mean zonal wind fields at 850 hPa. We focus on the 850 hPa winds because of the potential impact of surface winds on the oceans, and because the peak 850 hPa zonal winds is a common metric for defining the midlatitude eddy-driven jet (e.g., Banerjee et al., 2020; Grise & Polvani, 2014). Note that the climatological latitude of peak 850 hPa (eddy-driven jet) is poleward of the peak upper tropospheric winds (subtropical jet), and the eddy-driven and subtropical jets do not covary interannually and respond differently to increased CO_2 (Waugh et al., 2018).

Results are presented here for both zonal-mean winds, and for averages across the Pacific Ocean (150°E to 290°E) and the combined Atlantic-Indian Ocean (40°W to 120°E) sectors. Averages over the individual Atlantic and Indian produce similar results to the combined average, so we focus on the combined average for simplicity. We refer to the zonal winds averaged over the Pacific Ocean as "Pacific winds," and similarly winds averaged over the combined Atlantic-Indian Oceans as "Atlantic-Indian winds." For all longitudinal averages, the strength is defined as the magnitude of the peak winds in the SH, and the latitude is defined as the latitude at which this occurs. The latter is found in the gridded data by analytically fitting a quadratic

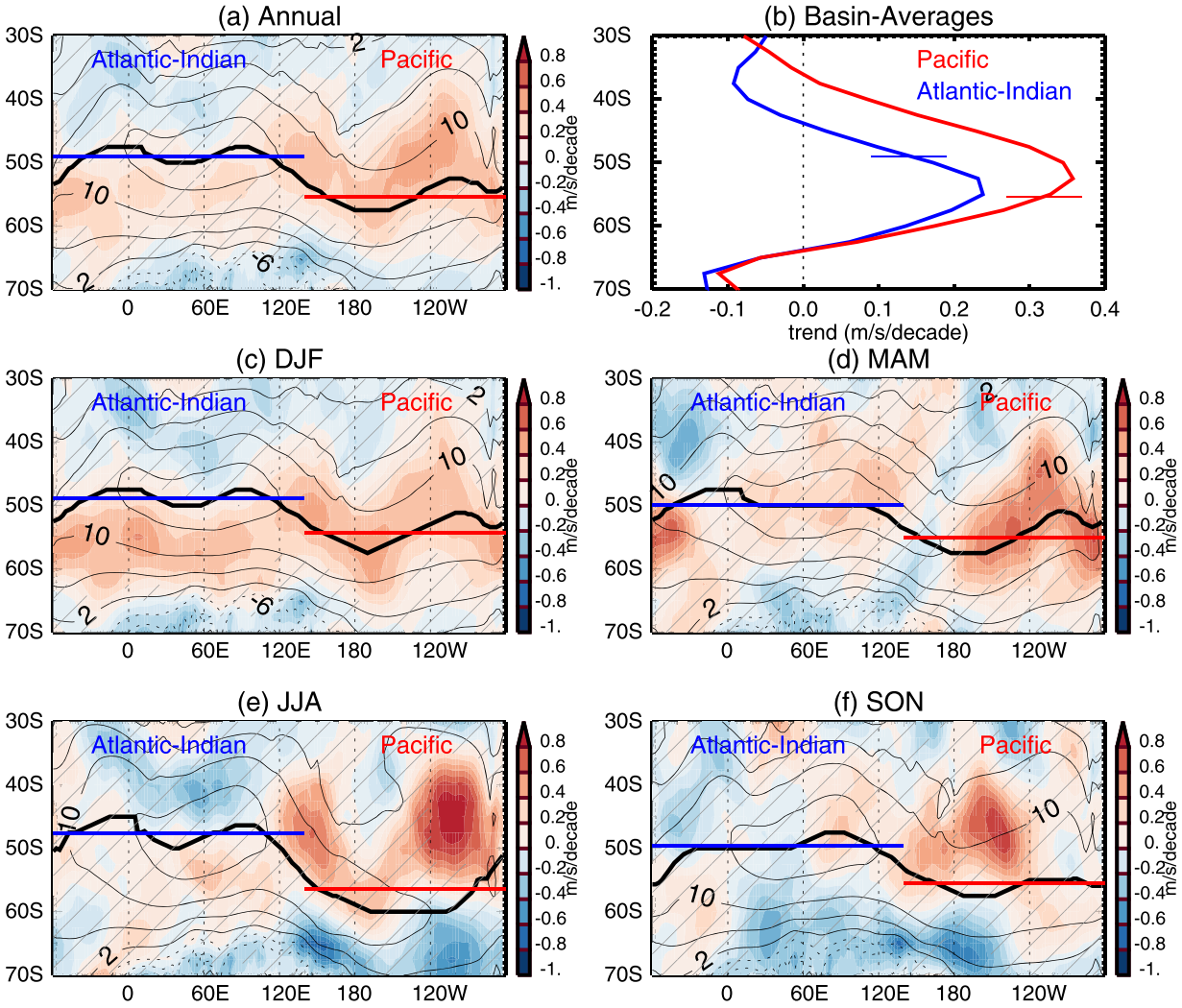

Figure 2. Maps of trends (colors) and climatology (contours) of 850 hPa zonal winds for 1980–2018 for (a) annual-mean, (c) DJF, (d) MAM, (e) JJA, and (f) SON, and (b) variations of trends in basin-average winds with latitude. Contours in panels (a) and (c)–(f) show climatological winds (interval of 2 m/s), thick curve shows climatological location of jet at each longitude, and horizontal lines show climatological-mean location of the Atlantic-Indian and Pacific jets. In panel (b) the horizontal bars show the climatological-mean location of the Atlantic-Indian and Pacific jets. All fields are based on the winds averaged over the three reanalyses. Gray hatching shows regions where wind trends are not statistically significant.

between the latitude of the grid with largest value and 10° either side. The results are not sensitive to the width used for the quadratic (not shown).

The statistical significance of the reanalysis trends is determined using the Student's t test with t statistic given by the estimated trend divided by the standard deviation. Following Swart et al. (2015), the uncertainty in the model ensemble mean trend (i.e., the forced trend) is represented by the (95%) confidence interval, which is given by $c\sigma/\sqrt{n}$, where n is number of models or members, σ^2 is the variance in trends across the ensemble members, and c is the 97.5th percentile of the Student's t distribution with $n-1$ degrees of freedom (von Storch & Zwiers, 1999). The spread among individual ensemble members is given the 2.5th to 97.5th percentiles of trends; this reflects the range due to internal variability, and also intermodel uncertainty for the multimodel ensembles.

3. Reanalyses

We begin by considering recent trends in the annual-mean winds, as these are likely the most relevant for driving changes in the oceans. We find good agreement among the meteorological reanalyses, see

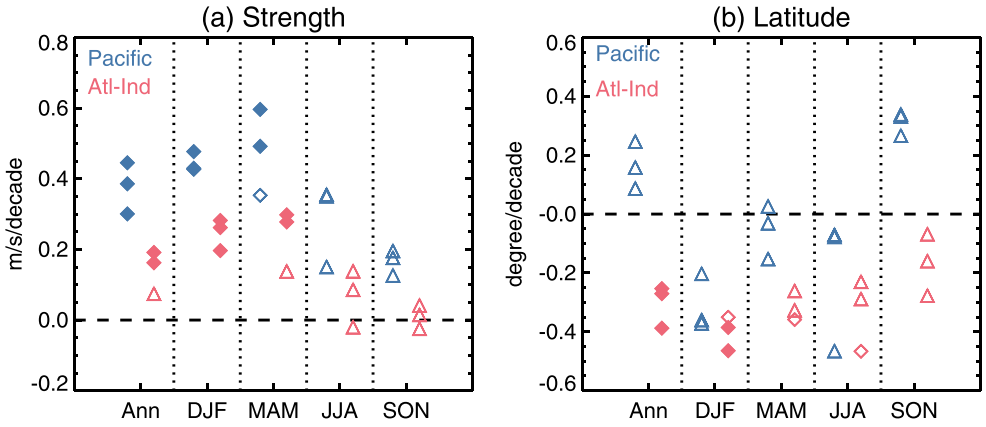

Figure 3. Seasonal variations in 1980–2018 trends in (a) strength and (b) latitude for Pacific (red) and Atlantic-Indian (blue) peak winds. Separate symbols for each of ERA, JRA55, and MERRA-55, with filled diamond indicating statistical significance at 95%, open diamond significant at 90%, and triangle not significant at 90%.

Figure 1. All reanalyses show an increase in the strength of the zonal-mean and in the basin-averaged winds, with the increase in the peak Pacific winds (linear trend of 0.3–0.45 m/s per decade across the reanalyses) being considerably larger than the increase of the Atlantic-Indian winds (0.1–0.2 m/s per decade), see Figures 1a–1c. The reanalyses also agree in showing an equatorward shift (0.1–0.25° per decade) in peak Pacific winds but a poleward shift (−0.25 to −0.4° per decade) in the Atlantic-Indian winds, see Figures 1e and 1f. The equatorward shift in the Pacific winds is statistically insignificant at the 95% confidence level, but the poleward shift of the Atlantic-Indian winds and the linear trend in difference between the latitude of peak Pacific and Atlantic-Indian winds (0.4–0.5° per decade) are statistically significant. In other words, there has been a differential movement of the peak Pacific and Atlantic-Indian winds over the last 40 years.

The different annual-mean trends between the Pacific and Atlantic-Indian winds are related to zonal asymmetries in *both* the climatological latitude of the peak winds and the wind trends. The climatological latitude of the peak annual-mean Pacific winds is poleward of the Atlantic-Indian winds (thick contour and horizontal lines in Figure 2a). At the same time the largest increase in winds occurs over the Pacific Ocean, and is equatorward of the regions of weak increases of the Atlantic and Indian oceans (Figure 2a). Larger trends over the Pacific than the other ocean basins are also found in satellite-based 10 m winds, see Figure 12 of Swart et al. (2015). As a result of these zonal variations, the largest zonal wind increase is equatorward of the peak winds over the Pacific sector (red curve in Figure 2b), yielding the equatorward (albeit not statistically significant) shift of the Pacific winds shown in Figure 1e. In contrast there is an increase in winds poleward of the peak Atlantic-Indian winds (blue curve in Figure 2b), resulting in the poleward shift of the peak Atlantic-Indian winds (Figure 1f).

The annual-mean strengthening of the winds shown in Figure 1 comes mainly from strengthening in December–February (DJF) and March–May (MAM) (Figures 2c–2f and 3a). However, there is strengthening all seasons (except for the Atlantic-Indian winds in September–November (SON)), and for all seasons the acceleration of the Pacific winds are stronger than that of the Atlantic-Indian winds (Figure 3a).

There is seasonality in zonal asymmetries in the trends in the latitude of peak winds (see Figure 3b). Although the trends in peak Pacific winds are not statistically significant, the sign of the trends change with season. There is a poleward shift of the Pacific winds in DJF, an equatorward shift in SON, and weak movement in other seasons (Figure 3b). Thus, the annual-mean equatorward shift of the Pacific winds is the residual between a spring equatorward shift and summer poleward shift. This seasonality is driven by changes in location and strength of the wind increase in the eastern Pacific (Figure 2). There is less seasonality for the latitude of the peak Atlantic-Indian winds, with a poleward shift found in all seasons (Figure 3b). However, as with the Pacific winds, the trend in latitude of Atlantic-Indian winds is more negative in DJF than in SON. Also, while the direction of Pacific winds shift differs seasonally, for all seasons, the reanalysis-mean Pacific winds shifts equatorward relative to the Atlantic-Indian winds.

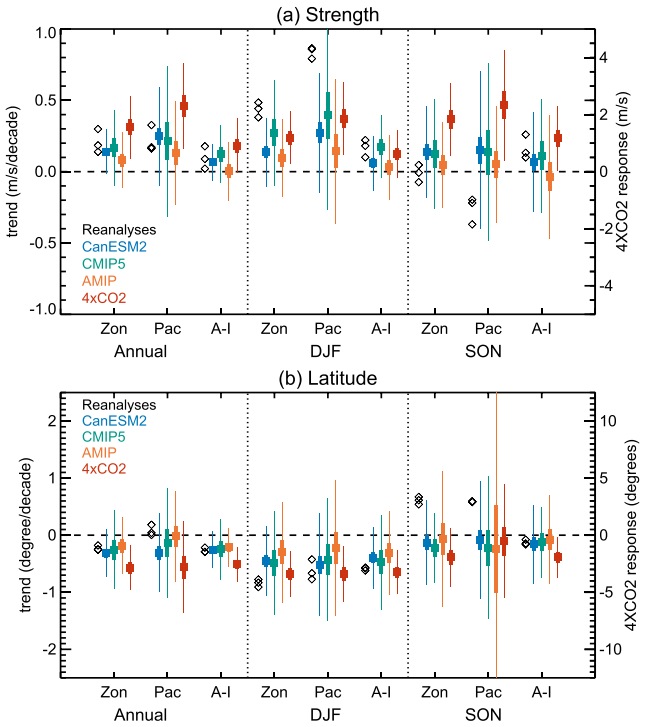

Figure 4. Trends in (a) strength and (b) latitude of peak winds for reanalyses (black), CanESM2 historical (blue), CMIP5 historical (green), CMIP5 AMIP (red), and CMIP5 4xCO2 (orange) ensembles. Trends are for 1980–2005 in reanalyses and models, except for 4xCO2 where difference between end of 4xCO2 simulations and PI simulation are shown (right axes). For the models the square shows the ensemble mean, thick vertical bar the 95% confidence interval on this mean, and thin bar the 2.5th to 97.5th percentiles of the trends. See Figure 3 for statistical significance of trends in reanalyses.

4. Climate Models

Several important questions arise from the above results. The primary question is whether the observed trends and their zonal asymmetries are a response to external forcing or merely internal variability. If the trends are a forced response, then a follow-on question is what is the actual forcing? Similarly, if internal variability, is this driven by SSTs or is it internal to the atmosphere? Answering these questions is critical for understanding how the SH climate might evolve in the future.

To answer these questions, we use the model ensembles described in section 2. Comparison of the historical and single-forcing simulations isolates the role of these different forcings, comparison of historical and AMIP simulations isolates the role of ocean-atmosphere coupling, and, lastly, comparison of the 4xCO2 and piControl simulations isolates the forced response to a large increase in CO_2.

Before addressing the issue of causality, we first determine whether the simulated all forcing historical trends and observed trends are consistent. Following Swart et al. (2015), we do this by determining whether the reanalysis trend falls within the 5th to 95th percentiles of the simulated trends. For both the CMIP5 and CanESM2 historical simulations, the reanalysis trends for basin-averaged winds fall within (or very close to) the model spread across all seasons for both the strength and the latitude of the winds, see Figure 4. (Note that in Figure 4 the trends for the models and reanalyses are calculated for 1980–2005, the common period between reanalyses and CMIP5 historical runs.) Thus, these climate models can simulate trends similar to those observed.

We now consider the cause of these trends. Extensive previous research has shown that stratospheric ozone depletion and increasing greenhouse gases (GHGs) have played the major role in the intensification and poleward shift of the zonal-mean winds in DJF (e.g., Banerjee et al., 2020; McLandress et al., 2011; Polvani et al., 2011). Analysis of the CMIP5 and CanESM2 ensembles support this, and also indicate this also applies for basin-averaged zonal winds. For both ensembles, models simulate a statistically significant ensemble-mean intensification and a poleward shift of the peak Pacific and Atlantic-Indian winds during DJF, with the vast majority of the individual simulations showing this intensification and poleward shift (Figure 4). This consistency in sign among simulations indicates that forcing has played a major contribution to DJF trends in basin-averaged winds.

The central role of ozone depletion and increases in GHGs in the DJF trends is further supported by analysis of the CanESM2 "single-forcing" ensembles (supporting information Figure S1): For all basins, there are near-zero (insignificant) ensemble-mean shifts in the NAT and AA simulations (e.g., for Pacific winds the shift is $0.07 \pm 0.1°$ per decade and $-0.02 \pm 0.1°$ per decade for the NAT and AA, respectively), which indicates that changes in solar forcing, volcanic eruptions, and anthropogenic aerosols are not the cause. However, there are significant ensemble-mean DJF trends for the OZ forcing ensemble ($-0.23 \pm 0.2°$ per decade), and for the GHG forcing estimated as residual between the historical and the sum of the single-forcing runs ($-0.33 \pm 0.3°$ per decade). Therefore, DJF trends in latitude of peak winds in the CanESM2 historical ensemble occur because of changes in stratospheric ozone and GHGs.

We now consider the spring (SON) trends. Less attention has been paid to trends in this season but, as shown above, the equatorward shift of the Pacific winds during this season dominates the annual-mean change. For both the CMIP5 and CanESM2 historical ensembles the ensemble-mean Pacific and Atlantic-Indian winds strengthen and shift poleward, although these ensemble-mean trends are not always statistically significant (Figure 4b). The sign of the ensemble-mean trends for the Atlantic-Indian winds agrees with the reanalyses,

but this is not the case for the Pacific winds, for which the reanalyses show a weakening and equatorward shift over the 1980–2005 period. However, for both metrics the spread in trends among the ensemble members is very large, and the observed trends lie within this spread. This suggests that the observed trends are not a forced response but result from internal variability. This interpretation is further supported by the CanESM2 single-forcing ensembles (supporting information Figure S1): For each single-forcing ensemble we find a similar large spread in shift in the SON peak Pacific winds across the 50 members and an insignificant ensemble-mean shift in the Pacific winds in SON ($0.18 \pm 0.2°$ per degree, $0.19 \pm 0.2°$ per degree, and $-0.15 \pm 0.3°$ per decade for the NAT, AA, and OZ ensembles, respectively).

The absence of a forced spring shift over the Pacific is supported by simulations that consider large increases in CO_2. Analysis of the CMIP5 $4xCO_2$ simulations shows a significant ensemble-mean poleward shift in the winds for all basins in DJF, but for SON the shift in the Pacific winds is not significant, see Figure 4b. In SON (and JJA) there is again a large spread among models, and half of the models show an equatorward movement. In other words, the shift in peak JJA and SON Pacific winds due to quadrupling of CO_2 is much less than intermodel variability, indicating that increases in CO_2 are unlikely to have caused the observed historical equatorward shift. There is, however, a significant winds strengthening in all seasons in the $4xCO_2$ simulations (Figure 4a and supporting information Figure S2). Thus, while increases in CO_2 over the rest of this century are unlikely to force a significant movement in SON Pacific winds, the simulations analyzed here suggest that it might lead to an overall strengthening of this winds.

Finally, we examine the question of whether the winter-spring trends, which we interpret as internal variability, are coupled to ocean variability. To address this, we compare the ensemble of CMIP5 historical simulations with the ensemble of CMIP5 AMIP simulations. Although all the CMIP5 AMIP simulations use the same observationally based SSTs, the spread in the shift in peak winds is comparable to, if not larger than, the historical simulations and AMIP simulations (see Figure 4b and supporting information Figure S2). Thus, internal atmospheric dynamics can generate large summer-spring trends in latitude of peak Pacific winds comparable to (and larger than) the observed trends. This conclusion that internal atmospheric variability plays an important role in multidecadal trends in peak winds is consistent with the Garfinkel et al. (2015) analysis of trends in the width of the Hadley Cell.

Returning to the questions posed at the start of this section, analysis of the above simulations indicates that the summer trends in magnitude and latitude of peak basin-average winds are due to changes in stratospheric ozone and GHGs, whereas the winter–spring trends in the latitude of the peak Pacific winds are not a forced response but are due to very large internal atmospheric variability.

5. Conclusions

It is well documented that meteorological reanalyses since 1979 show an increase in strength and poleward shift in the peak annual-mean near-surface winds in the SH, with the largest shift occurring in DJF (e.g., Swart & Fyfe, 2012; Thomas et al., 2015). Here we have shown that there are substantial longitudinal variations in the trends in both the strength and latitude of the near-surface winds. In the annual mean, the maximum winds strengthen in all basins, but the increase is larger over the Pacific than over the Indian and Atlantic Oceans. Furthermore, and perhaps more surprisingly, only over the Atlantic and Indian oceans have the peak zonal winds shifted poleward, with no significant shift over the Pacific Ocean. The differential movement of the annual-mean winds is caused by a spring equatorward shift over the Pacific that is much larger than the summer-fall poleward shift.

Previous studies (e.g., Banerjee et al., 2020; McLandress et al., 2011; Polvani et al., 2011) have shown that stratospheric ozone depletion and increasing GHGs have played the major role in the strengthening and poleward shift of the DJF zonal-mean winds. We find the same result for the basin-average winds. However, the simulations analyzed here indicate that winter-spring trends in the latitude of the peak Pacific winds are not a forced response but are due to very large internal variability. Furthermore, comparison of coupled and atmosphere-only simulations suggest this shift is due to internal atmospheric variability, rather than coupled atmosphere-ocean variability. The lack of a forced winter-spring shift in the Pacific winds extends to a quadrupling of CO_2. We have found a significant ensemble-mean poleward shift in the Pacific winds in DJF and MAM for $4xCO_2$ simulations, but not in JJA or SON. This suggest that increases

in CO_2—and other GHGs—over the rest of this century are also unlikely to force a significant movement of winter-spring peak winds over the Pacific.

Much of the research on trends in SH atmosphere and ocean circulation has emphasized the poleward shift of the westerlies. However, as shown here, over the Pacific sector, in winter and spring (and in the annual-mean) the westerlies have not shifted poleward and may have actually shifted equatorward. This will likely lead to different changes in storm tracks and precipitation, as well as in the ocean circulation, over the Pacific sector compared to other sectors. While these zonal differences in trends may only apply to winter-spring, the shift in annual-mean winds—and the longer response time of the oceans to wind forcing—may result in more persistent zonal asymmetries in ocean trends. For example, as the ocean gyre circulation responds to changes in basin-wide wind stresses, the different trends in Pacific and Atlantic-Indian winds suggest that trends in respective gyres may also differ. This then may result in zonal asymmetries in ocean ventilation, heat and carbon uptake, and sea level changes (e.g., Jones et al., 2019; Keppler & Landschützer, 2019; Waugh et al., 2019; Zhang et al., 2014).

Data Availability Statement

The reanalysis data sets can be downloaded from their respective webservers: The European Centre for Medium-Range Weather Forecasts (ECMWF) for ERA-I (https://apps.ecmwf.int/datasets/data/interim-full-daily/levtype=sfc/), the JMA Data Dissemination System (JDDS) for JRA-55 (https://jra.kishou.go.jp/JRA-55/index_en.html#download), and the Goddard Earth Sciences Data and Information Services Center (GES DIC) for MERRA2 (https://disc.gsfc.nasa.gov/datasets?keywords=%22MERRA-2%22&page=1&source=Models%2FAnalyses%20MERRA-2). The model output for CanESM2 can be accessed online (at http://climate-modelling.canada.ca/climatemodeldata/cgcm4/CanESM2/index.shtml), while the CMIP5data used in this study are freely available through the Earth System Grid Federation (https://esgf-node.llnl.gov).

Acknowledgments

We acknowledge the World Climate Research Programme's Working Group on Coupled Modelling, which is responsible for CMIP, and we thank the climate modeling groups for producing and making available their model output. We also acknowledge the Environment and Climate Change Canada's Canadian Centre for Climate Modeling and Analysis for executing and making available the CanESM2 Large Ensemble simulations used in this study. DWW and LMP are supported by grants from the U.S. National Science Foundation to Columbia University.

References

Banerjee, A., Fyfe, J. C., Polvani, L. M., & Waugh, D. W. (2020). A pause in Southern Hemisphere circulation trends due to the Montreal Protocol. *Nature*, *579*(7800), 544–548. https://doi.org/10.1038/s41586-020-2120-4

Barnes, E. A., & Polvani, L. (2013). Response of the midlatitude jets, and of their variability, to increased greenhouse gases in the CMIP5 models. *Journal of Climate*, *26*(18), 7117–7135. https://doi.org/10.1175/JCLI-D-12-00536.1

Cai, W., Cowan, T., Godfrey, S., & Wijffels, S. (2010). Simulation of processes associated with the fast warming rate of the southern mid-latitude ocean. *Journal of Climate*, *23*(1), 197–206. https://doi.org/10.1175/2009JCLI3081.1

Dee, D. P., Uppala, S. M., Simmons, A. J., Berrisford, P., Poli, P., Kobayashi, S., et al. (2011). The ERA-Interim reanalysis: Configuration and performance of the data assimilation system. *Quarterly Journal of the Royal Meteorological Society*, *137*(656), 553–597. https://doi.org/10.1002/qj.828

Eichelberger, S. J., & Hartmann, D. L. (2007). Zonal jet structure and the leading mode of variability. *Journal of Climate*, *20*(20), 5149–5163. https://doi.org/10.1175/JCLI4279.1

Fogt, R. L., & Marshall, G. J. (2020). The Southern Annular Mode: Variability, trends, and climate impacts across the Southern Hemisphere. *Wiley Interdisciplinary Reviews: Climate Change*, *11*(4). https://doi.org/10.1002/wcc.652

Gagné, M.-È., Fyfe, J. C., Gillett, N. P., Polyakov, I. V., & Flato, G. M. (2017). Aerosol-driven increase in Arctic sea ice over the middle of the twentieth century. *Geophysical Research Letters*, *44*, 7338–7346. https://doi.org/10.1002/2016GL071941

Garfinkel, C. I., Waugh, D. W., & Polvani, L. M. (2015). Recent Hadley cell expansion: The role of internal atmospheric variability in reconciling modeled and observed trends. *Geophysical Research Letters*, *42*, 10,824–10,831. https://doi.org/10.1002/2015GL066942

Gelaro, R., McCarty, W., Suárez, M. J., Todling, R., Molod, A., Takacs, L., et al. (2017). The Modern-Era Retrospective Analysis for Research and Applications, version 2 (MERRA-2). *Journal of Climate*, *30*(14), 5419–5454. https://doi.org/10.1175/JCLI-D-16-0758.1

Grise, K. M., Davis, S. M., Simpson, I. R., Waugh, D. W., Fu, Q., Allen, R. J., et al. (2019). Recent tropical expansion: Natural variability or forced response? *Journal of Climate*, *32*(5), 1551–1571. https://doi.org/10.1175/JCLI-D-18-0444.1

Grise, K. M., & Polvani, L. M. (2014). Is climate sensitivity related to dynamical sensitivity? A Southern Hemisphere perspective. *Geophysical Research Letters*, *41*, 534–540. https://doi.org/10.1002/2013GL058466

Grise, K. M., & Polvani, L. M. (2016). Is climate sensitivity related to dynamical sensitivity? *Journal of Geophysical Research: Atmospheres*, *121*, 5159–5176. https://doi.org/10.1002/2015JD024687

Hall, A., & Visbeck, M. (2002). Synchronous variability in the Southern Hemisphere atmosphere, sea ice, and ocean resulting from the annular mode. *Journal of Climate*, *15*(21), 3043–3057. https://doi.org/10.1175/1520-0442(2002)015<3043:SVITSH>2.0.CO;2

Hendon, H. H., Thompson, D. W., & Wheeler, M. C. (2007). Australian rainfall and surface temperature variations associated with the Southern Hemisphere annular mode. *Journal of Climate*, *20*(11), 2452–2467. https://doi.org/10.1175/JCLI4134.1

Jones, D. C., Boland, E. J., Meijers, A. J. S., Forget, G., Josey, S. A., Sallee, J.-B., & Shuckburgh, E. (2019). Heat distribution in the Southeast Pacific is only weakly sensitive to high-latitude heat flux and wind stress. *Journal of Geophysical Research: Oceans*, *124*, 8647–8666. https://doi.org/10.1029/2019JC015460

Keppler, L., & Landschützer, P. (2019). Regional wind variability modulates the Southern Ocean carbon sink. *Scientific Reports*, *9*(1), 1–10.

Kobayashi, S., Ota, Y., Harada, Y., Ebita, A., Moriya, M., Onoda, H., et al. (2015). The JRA-55 Reanalysis: General specifications and basic characteristics. *Journal of the Meteorological Society of Japan. Ser. II*, *93*(1), 5–48. https://doi.org/10.2151/jmsj.2015-001

Le Quere, C., Rödenbeck, C., Buitenhuis, E. T., Conway, T. J., Langenfelds, R., Gomez, A., et al. (2007). Saturation of the Southern Ocean CO_2 sink due to recent climate change. *Science*, *316*(5832), 1735–1738. https://doi.org/10.1126/science.1136188

McLandress, C., Shepherd, T. G., Scinocca, J. F., Plummer, D. A., Sigmond, M., Jonsson, A. I., & Reader, M. C. (2011). Separating the dynamical effects of climate change and ozone depletion. Part II: Southern Hemisphere troposphere. *Journal of Climate*, *24*(6), 1850–1868. https://doi.org/10.1175/2010JCLI3958.1

Polvani, L. M., Waugh, D. W., Correa, G. J. P., & Son, S.-W. (2011). Stratospheric ozone depletion: The main driver of twentieth-century atmospheric circulation changes in the Southern Hemisphere. *Journal of Climate*, *24*(3), 795–812. https://doi.org/10.1175/2010JCLI3772.1

Roemmich, D., Gilson, J., Davis, R., Sutton, P., Wijffels, S., & Riser, S. (2007). Decadal spinup of the South Pacific subtropical gyre. *Journal of Physical Oceanography*, *37*(2), 162–173. https://doi.org/10.1175/JPO3004.1

Schneider, D. P., Deser, C., & Fan, T. (2015). Comparing the impacts of tropical SST variability and polar stratospheric ozone loss on the Southern Ocean westerly winds. *Journal of Climate*, *28*(23), 9350–9372. https://doi.org/10.1175/JCLI-D-15-0090.1

Sen Gupta, A., & England, M. H. (2006). Coupled ocean–atmosphere–ice response to variations in the southern annular mode. *Journal of Climate*, *19*(18), 4457–4486. https://doi.org/10.1175/JCLI3843.1

Swart, N. C., & Fyfe, J. C. (2012). Observed and simulated changes in the Southern Hemisphere surface westerly wind-stress. *Geophysical Research Letters*, *39*, L16711. https://doi.org/10.1029/2012GL052810

Swart, N. C., Fyfe, J. C., Gillett, N., & Marshall, G. J. (2015). Comparing trends in the Southern Annular Mode and surface westerly jet. *Journal of Climate*, *28*(22), 8840–8859. https://doi.org/10.1175/JCLI-D-15-0334.1

Taylor, K. E., Stouffer, R. J., & Meehl, G. A. (2012). An overview of CMIP5 and the experiment design. *Bulletin of the American Meteorological Society*, *93*(4), 485–498. https://doi.org/10.1175/BAMS-D-11-00094.1

Thomas, J. L., Waugh, D. W., & Gnanadesikan, A. (2015). Southern Hemisphere extratropical circulation: Recent trends and natural variability. *Geophysical Research Letters*, *42*, 5508–5515. https://doi.org/10.1002/2015GL064521

Thompson, D. W., Solomon, S., Kushner, P. J., England, M. H., Grise, K. M., & Karoly, D. J. (2011). Signatures of the Antarctic ozone hole in Southern Hemisphere surface climate change. *Nature Geoscience*, *4*, 741–749. https://doi.org/10.1038/ngeo1296

Thompson, D. W. J., & Wallace, J. M. (2000). Annular modes in the extratropical circulation: I. Month-to-month variability. *Journal of Climate*, *13*(5), 1000–1016. https://doi.org/10.1175/1520-0442(2000)013<1000:AMITEC>2.0.CO;2

Toggweiler, J. R., & Russell, J. (2008). Ocean circulation in a warming climate. *Nature*, *451*(7176), 286–288. https://doi.org/10.1038/nature06590

von Storch, H., & Zwiers, F. W. (1999). *Statistical analysis in climatology*. Cambridge University Press.

Waugh, D. W., Grise, K. M., Seviour, W. J. M., Davis, S. M., Davis, N., Adam, O., et al. (2018). Revisiting the relationship among metrics of tropical expansion. *Journal of Climate*, *31*(18), 7565–7581. https://doi.org/10.1175/JCLI-D-18-0108.1

Waugh, D. W., & Haine, T. W. N. (2020). How rapidly do the southern subtropical oceans respond to wind stress changes? in revision. *Journal of Geophysical Research: Oceans*, *125*, e2020JC016236. https://doi.org/10.1029/2020JC016236

Waugh, D. W., McC. Hogg, A., Spence, P., England, M. H., & Haine, T. W. N. (2019). Response of Southern Ocean Ventilation to Changes in Midlatitude Westerly Winds. *Journal of Climate*, *32*(17), 5345–5361. https://doi.org/10.1175/jcli-d-19-0039.1

Waugh, D. W., Primeau, F., DeVries, T., & Holzer, M. (2013). Recent changes in the ventilation of the southern oceans. *Science*, *339*(6119), 568–570. https://doi.org/10.1126/science.1225411

Yang, D., Arblaster, J. M., Meehl, G. A., England, M. H., Lim, E. P., Bates, S., & Rosenbloom, N. (2020). Role of tropical variability in driving decadal shifts in the Southern Hemisphere summertime eddy-driven jet. *Journal of Climate*, to appear, *33*(13), 5445–5463. https://doi.org/10.1175/JCLI-D-19-0604.1

Zhang, X., Church, J. A., Platten, S. M., & Monselesan, D. (2014). Projection of subtropical gyre circulation and associated sea level changes in the Pacific based on CMIP3 climate models. *Climate Dynamics*, *43*(1–2), 131–144. https://doi.org/10.1007/s00382-013-1902-x